NON-DESTRUCTIVE TESTING OF CHALLENGING AEROSPACE STRUCTURES

G. Jacob*, J. Tuppatsch*, D. Schmidt†, A. Pototzky†, R. Rodeck*, F. Raddatz*, G. Wende*

* German Aerospace Center (DLR), Institute of Maintenance, Repair and Overhaul, Hein-Sass-Weg 22, 21129 Hamburg, Germany

† German Aerospace Center (DLR), Institute of Lightweight Systems, Lilienthalplatz 7, 38108 Braunschweig, Germany

Abstract

High-performance multi-functional structures such as composites with integrated sensors for Structural Health Monitoring (SHM) or with integrated electrical conductor tracks are promising technologies for lightweight aerospace design. The reliability and performance of these challenging aerospace structures are ensured by suitable inspection and maintenance. However, the inspection of such structures via conventional Non-Destructive Testing (NDT) methods encounters challenges for the accurate damage detection, localization and characterization. In case of structural damages, using multiple NDT methods can ensure an efficient damage assessment. Key challenges to be solved are the proper selection of complementary and applicable NDT methods, the information content and quality about the structure which can be obtained by a single method, and the combined achievable information quality.

In this research, Carbon Fiber Reinforced Polymer (CFRP) specimens with bonded conductor tracks with artificially created defects and bonded piezoelectric lead zirconate titanate (PZT) sensors are considered. The composite specimens with bonded PZT sensors are impacted with different impact energy levels to create a variety of typical defects. The electro-mechanical impedance spectroscopy is used to study the adhesion of the PZT sensors to the composite specimens before and after impacts. The composite specimens are inspected using ultrasonic testing and thermography testing before and after impacts. The specific focus is on the assessment of the performance of each NDT method for damage detection in the presence of integrated functional elements. Both NDT methods are suitable for the inspection and show good performance for damage assessment. The presence of the functional elements, however, affects the quality of the damage assessment. The sensitivity of the NDT methods for a precise identification of size and depth of defects is reduced. Ultrasonic testing provides a better spatial resolution in detecting the subsurface defects as well as the size and depth of defects. Thermography is effective in detecting defects closer to the surface, but provides less detailed information about the depth of the defects compared to the ultrasonic testing. This suggests that the combination of information using suitable data formats is relevant in order to make informed decisions about a structure. Digital Imaging and Communication for Nondestructive Evaluation (DICONDE) is discussed as a potential standard data format for the exchange and fusion of NDT data from various methods.

Keywords

composite structure; non-destructive testing; structural health monitoring; ultrasonic testing; defect detection; inspection; thermography

1. INTRODUCTION

One of the measures highlighted by the European Commission's "Destination 2050 – A route to net zero European aviation"[1] for CO_2 reduction and sustainable aviation is the reduction of fuel consumption by weight reduction technologies. Composite materials for large structures (aircraft fuselage or storage tanks for rockets or large wind turbine nacelles) such as Carbon Fiber Reinforced Polymer (CFRP) or Glass Fiber Reinforced Polymer (GFRP) have gained significance and widespread adoption due to their exceptional strength-to-weight ratio while ensuring exceptional or enhanced mechanical performance compared to conventional materials [1,2]. In a similar manner, the use of multi-functional structures such as composites with functional elements like integrated electrical conductive tracks, sensors for Structural Health Monitoring (SHM), actuators, fiber-optic sensors (FOS), antennas, lightning mesh, heating elements or printed circuit boards (PCBs) presents a promising approach for reducing weight and at

[1] https://www.destination2050.eu/

doi: 10.25967/630245

the same time providing functionalities beyond their structural application [3–5].
Despite the advantages and promising application, ensuring the reliability and safety aspects through Maintenance, Repair and Overhaul (MRO) of these multi-functional composite structures with integrated functional elements is the most important aspect that could further improve their system integration [6]. Non-Destructive Testing (NDT) methods such as visual testing (VT), ultrasonic testing (UT), Eddy-current testing (ECT), thermography testing (TT) and X-ray are suitable for the the inspection of composite structures [7–9]. However, all NDT methods have their own sensitivities with regard to damage characterisation and are very specialized for different types of structures and material combinations. Additionally, the selection of NDT methods depends on factors such as the geometry of the structure, inspection speed, size of damages and the accessibility for inspections. Thereby, the use of different NDT methods may be important for obtaining additional information about the structure and has proven to be very effective in numerous applications.
The proper selection of complementary and applicable NDT methods for the optimal damage detection and condition monitoring can effectively address the specific inspection requirements as well as improve existing methods [1]. Additionally, the information in a single inspection method, the combined achievable information from multiple methods and the integration of NDT data are important for minimizing uncertainties and improve the inspections and thus optimizing maintenance processes.
In this study composite specimens with piezoelectric lead zirconate titanate (PZT) transducers and conductor tracks which are bonded to the structure are considered. NDT is used to determine the presence of any preexisting flaws, their location and the varying characteristics for each NDT method. The prepared specimens are then subjected to multiple impacts with energies predetermined via pretests. The performance of each NDT method, i.e. UT through transmission technique, UT pulse echo technique and TT for characterisation of the specimens due to impact damages are investigated.
In the following sections, first a short literature review is presented (section 2). Later, the specimens used, the impact method used as well as the NDT methods are described (section 3). In (section 4)), the results of the NDT before and after impact damages are described and discussed including the strengths and weaknesses of each NDT method, followed by the conclusion (section 5).

2. INSPECTION OF COMPOSITE STRUCTURES WITH FUNCTIONAL ELEMENTS

The advantages of CFRP and GFRP due to their exceptional light-weight properties are well explored in the research with regard to understanding the damage mechanisms in structures without functional elements. The primary damage modes identified and investigated by most articles include matrix cracking, delamination, fibre breakage, debonding and buckling of fibres TAB 1. Impact-induced delamination is identified as the most common failure mode [1, 7]. The effects of impact also vary depending on the severity of the impact (velocity, impactor geometry, energy level) and location. Similarly, the use of different types of sensors for SHM is well explored. However, in order to limit the scope of the research, in the following section only composite structures with functional elements are considered.

Material	Structure	Tests	NDT methods	Reference
PZT	CFRP	fatigue	Micrographs	[10]
PZT	GFRP	Impacts	PZT, UT, TT, vibration	[11]
PZT	CFRP	tensile, fatigue, impact	UT	[12]
FOS	CFRP	deformation	X-ray	[13]
Copper	CFRP	tensile	Micrographs, Conductivity	[14]
Copper	CFRP, GFRP	compression	FEA	[15]
Copper	CFRP, GFRP	fatigue	X-ray, UT	[16]
Copper	CFRP, GFRP	fatigue	X-ray, VT, UT	[17]
Copper	GFRP	Impact	X-ray, SEM	[18]

TAB 1. Overview of failure studies on composites with embedded metal strips, foils or films

2.1. Structures with sensor patches

Embedded and integrated strain sensors, such as FOS, fiber Bragg grating (FBG) and PZT sensors find their application in monitoring damage events or impacts when the structure is in operation. Most studies in this field therefore focus on the performance and functionality of the embedded or bonded sensor patches to detect and monitor different types of damages [19, 20], to study the structural performance [21], to determine the damage propagation under different types of loading [12] or to determine the durability of the embedded sensors under fatigue loading [10]. Bending tests, fatigue tests and impact tests are used to identify the reliability and failure mechanisms in structures with embedded PZT. The studies conclude that the integration of sensor patches into host material can yield different outcomes regarding the tensile and compressive strength of the composite material due to their material properties and operational mechanisms. FOS presents a lower risk of negatively impacting the composite's structural integrity compared to PZT sensors. The sensors must be more durable than the structures and emphasizes their critical role in maintaining performance.

2.2. Structures with conductors

Compared to the research trend on structures with embedded sensors, structures with other functional elements have only been sparsely considered. Metal, especially copper, is favoured as the material for integrating conductor tracks inside the composites due to its excellent conducting properties and low electrical

resistivity [16,22]. The most common types of damage reported are debonding failures between the copper and composite and cracks which are detected by multiple NDT methods. The fatigue tests conducted by [17] on "dog bone" shaped specimens with embedded and surface-mounted copper foils indicate that embedded copper foil had more fatigue life than surface-mounted copper foils.
There is a need to focus on in-service damages and particularly the effects of inspection of structures with functional elements. The damages that occur for this type of structures could be analysed using different NDT methods. Although the NDT methods are effective to characterise damages, the factors such as accessibility and sensitivity to characterise smart structures are yet to be investigated. Thus, the suitability of each NDT method could be determined for well-informed decision making during the inspection process.

3. MATERIALS AND METHODS

3.1. CFRP specimens and impact damage

The focus of the experiments in this paper is to investigate the suitability of different NDT methods for the inspection of composite structures with different functional elements subjected to impact tests. Copper metallic foils used as electrical conductor tracks and ultrasonic transducers (DuraAct[2]) used for SHM systems are considered in this research as functional elements. The CFRP specimens considered here are 20 CFRP coupon specimens made from Hexcel's M21 prepreg material with a quasi-isotropic layer structure [23]. The dimensions of the specimens correspond to the American Society for Testing and Materials (ASTM) D7137 Compression after impact (CAI) sample size (150 mm x 100 mm x 3.3 mm size). Piezocomposite transducers were bonded at the centre of 14 specimens using a Loctite Hysol adhesive (FIG 1(a)). Similarly, conductor tracks are bonded to two other specimens. One of them is bonded incorrectly to provide an artificial damage before impact tests. The specimen 22_01010 consists of two bonded conductor tracks of which one strip is contaminated by a fingerprint and a left over part of the protective adhesive film of the conductor track (FIG 1). The other conductor track strip is artificially damaged using a drop of release agent (later removed using a cloth). Four of the CFRP specimens without integrated elements are used as reference for impact energy determination.
A mobile impact cannon is used to introduce impact damage of varying intensity into the test specimen. The impact projectile weighs 0.8253 kg and features a hemispherical head with a diameter of 16 mm. The appropriate range of impact energies is defined with the help of pretests. The energy is gradually increased until damage is recognisable via NDT. The settings of the impact cannon only allow a minimum energy of

[2] https://www.piceramic.com/en/products/piezoceramic-actuators/patch-transducers/

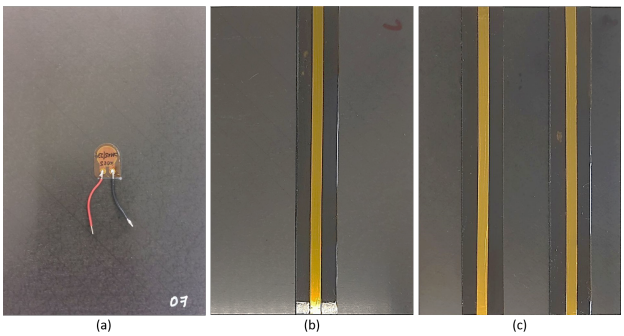

FIG 1. Composite specimen with (a) bonded PZT, (b) one bonded conductor track and (c) two bonded conductor tracks with artificial defects.

8.5 J. Therefore this is chosen as the minimum energy for the specimens with functional elements. The maximum energy is chosen as 18 J considering the fact that this is enough to induce the required damage to the specimen. All other specimens are then subjected to impacts based on these criteria falling between minimum and maximum energy. The impacts are made directly on the opposite side of the specimen to which the PZT transducers are bonded. Different impact locations are chosen: next to the PZT transducer, with a slight overlap to the PZT transducer and directly colocated with the transducer. The aim of the tests is to detect detachment between the functional elements such as the metal foils or PZT patches from the specimens as well as delaminations within the specimen. This is particularly challenging because the damage information may interfere with the influence of the functional element in the NDT data, which also appears in undamaged samples.

3.2. Inspection methods

The following NDT methods are employed to particularly investigate the effect of impacts on functional elements. Accompanying the NDT, the sensors are measured using impedance spectroscopy to check for detachment and damage to the ceramic transducers. The ability of the sensors to detect damage is not tested. The experiments focused on the functionality of the individual sensors with respect to an impact.

3.2.1. Impedance Spectroscopy

Electro-Mechanical Impedance (EMI) analysis using a Cypher Instruments C60 impedance analyzer is utilised to test the detachment and bonding of PZT to the specimens [24, 25]. An electrical voltage, which is applied between the two opposite circular surfaces of the transducer, leads to a deformation of the transducer perpendicular to the lines of the electrical field. In the free state, the ceramic in the transducer deforms according to the applied electrical voltage. In the case of an alternating voltage, the ceramic begins to vibrate. The course of the electrical impedance over the excitation frequency indicates the vibration

behaviour as well as the mechanical and electrical integrity and bonding of the ceramic. In the case of free oscillation, impedance and phase show characteristic deflections. In the application of PZT sensors for the SHM of structures, the impedance analysis is also used as a self-test for testing the functionality and bonding of the transducers. The EMI spectrum is considered in this experiment as a reference value for identifying different anomalies with regard to the individual PZT transducers as well as the bonding of the transducer to the structure.

3.2.2. Ultrasonic testing

The composite specimens are inspected before damage and after damage via UT using a Hillger NDT system with immersion technique. The USPC imaging systems in the through transmission configuration and pulse-echo configuration is used to inspect all the probes before impacts to identify the predamage state and the artificial defects in the specimens 21 and 22. The scanning spatial resolution is set to 0.25 mm per pixel. The signal obtained in through transmission method (C-Scan) as well as the damage echo, the damage depth and back-wall echo in pulse-echo mode are plotted for the effective visualisation of the inspection.

3.2.3. Thermography

The specimen are inspected via lock-in thermography in reflection mode using a FLIR bolometer camera. The specimens are thermally excited (sinusuidal, uncalibrated) using infrared radiation emitters with an emission wavelength range close to 1.1 µm. The modulation frequency of the sinusoidal heat wave is varied between 0.02 Hz and 0.16 Hz and the camera captures images at a frequency of 10 Hz ± 0.2 Hz. Direct Fourier Transform (DFT) is used to analyze the collected temperature data. With the developed TT system, it is expected to record anomalies up to 5 mm in the amplitude image and 5 mm in the phase image. The specimens are inspected from both sides i.e. the front side with the functional element and the back side.

4. RESULTS AND DISCUSSION

4.1. Inspections before impacts

In general, UT using the through-transmission and pulse-echo configuration indicate a flaw-free condition for all the specimens with PZT patches and indicate the PZT transducers and their components in each inspection (FIG 2). The solder joint for the electrical contact of the DuraAct transducer, the piezoceramic layer with the electrode and the polymer layer for electrical insulation are visible via both UT methods. The differences in the measurements are that the wires for the EMI measurements are visible only in the through transmission echo and that the extend of bonding of the patch to the specimen is better visible in the backwall echo scan from UT pulse echo methods. This information about the bonding of the PZT patches to the specimen varies from specimen to specimen. It should be noted here that the wires used for EMI measurements do not represent a proper solution for real integrated functional elements. The EMI measurement confirmes the variation in bonding of the PZT patch to the specimen. The front side TT inspection covers the entire PZT transducer as well as the the entire structure, the electrodes with the piezoceramic layer and the electrical contacts. However the back side inspection only indicates a slight variation due to the presence of the PZT transducers and cannot characterise the different aspects of the PZT transducers in detail.

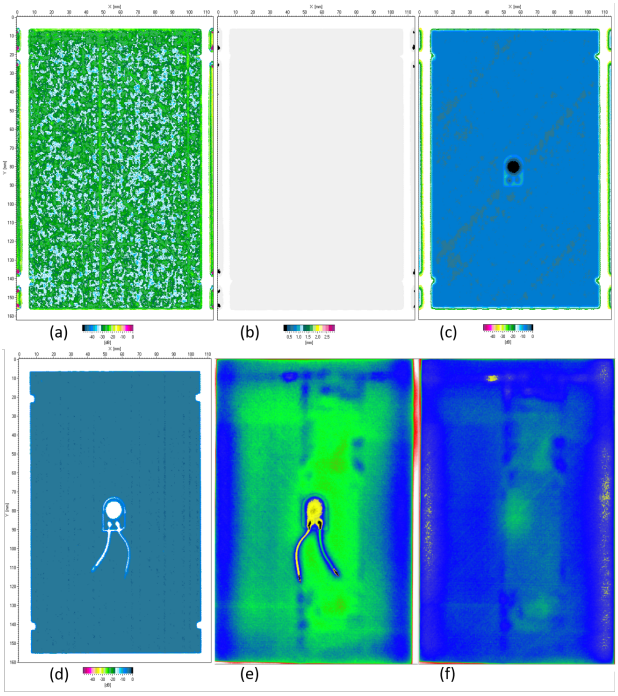

FIG 2. NDT results for specimen 07 showing the PZT (a) pulse-echo amplitude scan, (b) pulse-echo damage depth scan, (c) pulse-echo backwall scan, (d) through-transmission C-scan, (e) thermography from transducer side and (f) thermography from the back side

For specimen 21_00100 the used NDT methods show no artificial defects or any other defects. Similarly for the specimen 22_01010, no defects are observed using the UT pulse echo technique. However, UT through transmission technique reveals the artificial defect due to the adhesive protective film. The defect due to the drop of the release agent is slightly recognizable upon careful examination but the artificial defect due to the fingerprints are not clearly detectable (FIG 4). Double sided access is crucial for this application and influence the inspection results for a precise characterisation of the composite structure.

4.2. Inspections after impacts

In general the visual inspection using a magnifying glass reveals cracks in the polymer layer surrounding

Num.	Specimen Id.	Functional element	Impact energy (J)	Impact position	Criteria
7	07_15274	PZT	9.9	on	EMI unchanged
9	09_15138	PZT	13.4	on	EMI over free state
10	10_15154	PZT	15.5	on	PZT debonded
12	12_15115	PZT	10.9	above	EMI unchanged
16	16_15112	PZT	16.7	overlap	EMI between
17	17_15265	PZT	18.3	overlap	EMI over free state

TAB 2. Comparative analysis of selected specimens in terms of impact energy and location of impacts and EMI measurements

the PZT sensor for all the specimens with transducers as the functional element. The cracks vary from transducer to transducer and no trend can be observed, given the limited sample size. The energy of 8.9 J has an effect on the applied piezoelectric transducer. This can be seen in the EMI spectrum, but does not cause the piezoelectric sensors to completely detach from the sample plate. For three specimens, in which the impact is directly colocated with the transducer, the PZT transducers disbond from the structure. This can be attributed to the variation in manual bonding using the adhesive. Thus 13.4 J is the maximum energy for this experimental phase for direct impacts at the center of the specimen. However, the functionality of none of the transducers is affected as indicated by the EMI measurements after the impacts.

The EMI spectrum varies according to the impact energy. All impacts lead to a change in the EMI spectrum. The higher impact energies (13.39 J and 18.27 J) have a strong influence and lower impact energies (9 J) have a lower influence on the EMI spectrum. A shift in the spectrum can also be seen depending on the impact energies (FIG 3). The specimens 07_15274, 09_15138, 10_15154, 12_15115 and 17_15265 are chosen for a more detailed comparative analysis of the samples. The criteria from TAB 2 are used for the selection.

FIG 3 is the inspection results and following is a detailed discussion of the inspections of the respective specimens with regard to the different NDT methods:

- **Specimen 07_15274**: The VT revealed only matrix cracking (≈7.5mm) at the outer region. The UT tests reveals the impact directly on the transducer as well as the components of the PZT transducer. The damage morphology via UT through transmission method reveals some more artifacts closer to the solder joints as opposed to the damage and backwall scans generated by UT pulse echo method. It is also observed that no information about the damage depth could be deduced from the UT pulse echo data. It can only be deduced from the TT that a transducer might have been applied to the rear end of the structure. The impact had only slightest influence (closer to intact) on the EMI measurements. However, not information about the bonding of the specimens could be drawn from the three NDT methods.
- **Specimen 09_15138**: The lines indicating fiber break/matrix crack were revealed in the VT. The UT data indicates a direct impact of 13.4J below the transducer. The morphology of the damage are different for both the UT methods. The damage depth could be deduced from the UT pulse echo method to be at a maximum of 1mm. It can be seen from the TT on the transducer side that the heat flow in the centre of the transducer has changed significantly compared to the flaw-free state. Only small but some anomalies without much details including the bonded transducer can be seen for the inspections from the back side of the specimen. As a result of the impact, the impedance and phase angle has moved ahead of the free state. The reason might be due to the impact and thereby variation in the vibration behaviour of the piezoceramic layer.
- **Specimen 10_15154**: The 15.5J impact energy made the sensor to be completely detached from the specimen. The VT revealed only fiber break in the form of a line (≈11.24mm). The UT data reveals similar damage morphology for both techniques including the debonding of the transducer from the specimen. The damage depth reveals a damage from the surface upto a depth of 3mm from the surface. Two heat flow anomalies are observed in the TT data equally for inspections from either sides and thus a good correlation can be observed. As a result of the detachment of the transducer, the impedance phase is more similar to that of the free state of the transducers.
- **Specimen 12_15115**: The 10.9J impact could not make any indentation and only lines indicating fiber break could be observed. The UT data indicated the impact above the transducer and also all the different components of the transducer. Additionally, the slight detachment of the transducer from the structure can also be observed. Two heat flow anomalies can be observed from the TT data from the transducer side of the specimen. No damage anomalies can be seen via TT from the opposite side of the transducer. The EMI measurement has only slight shift caused due to the slight detachment of the transducer from the structure.
- **Specimen 16_15112**: The 16.7J impact created visible indentation and fiber breakage (≈8.60mm) in the specimen. The specimen was still intact and no visible indications of debonding was observed via VT. The UT data reveals an impact adjacent to the transducer but the slight detachment of the transducer can also be observed in both UT techniques. Two heat flow anomalies are observed in the TT data from the transducer side of the specimen. Only one clear anomaly can be observed from the opposite side of the specimen. The damage morphology is different for all the three NDT methods. After the impact, the impedance phase lies between the free and undamaged state.
- **Specimen 17_15265**: The impact results in indentation and two lines (≈5mm) of fiber break at the surface of the specimen. Both the UT methods reveals the impact adjacent to the transducer. The bond of the structure to the transducer on one

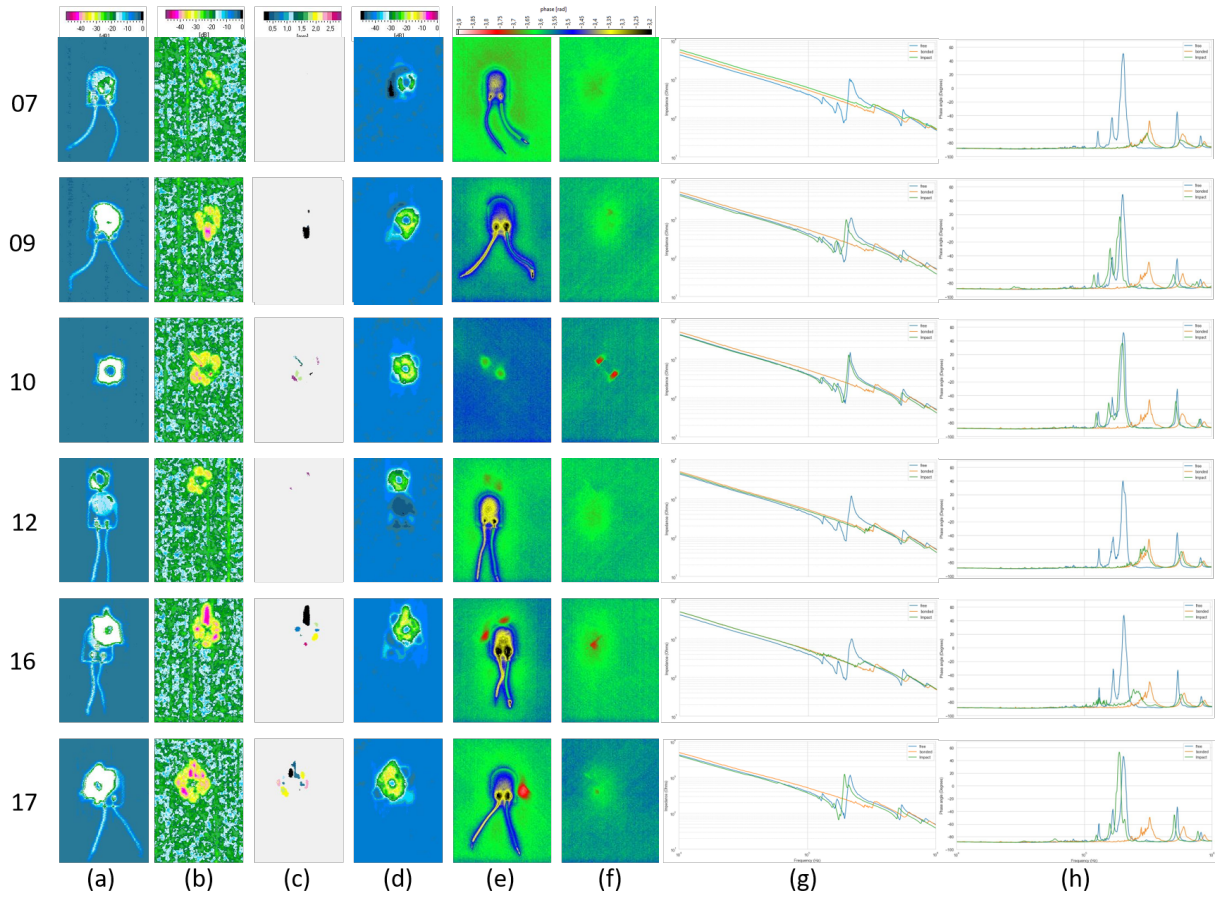

FIG 3. Inspection for selected specimens with PZT (a) through-transmission C-scan, (b) pulse-echo amplitude scan, (c) pulse-echo damage depth scan, (d) pulse-echo backwall scan, (e) TT from transducer side, (f)TT from back side (g) Impedance (Ohm) and (h)phase angle (°)

side can be observed in the UT through transmission data. However, the damage covers the other side of the transducer. The damage morphology however are different for both the UT methods. A large heat flow anomaly is revealed via TT on the transducer side of the specimen. However only a small damage is observed from the opposite side of the transducer. After the impact, the impedance phase indicates measurements close to free state of the transducer. Here, the both the EMI and TT validate a partial detachment of the transducer from the specimen.

In case of specimens 21_00100 and 22_01010, indentation and lines (≈11mm) are observed on the surface due to the 17.8J and 10.4J impact respectively. The impact damage including the indentation due to the projectile are visible in both the UT methods (FIG 4). Though, the damage echo scan indicates a damage in the case of 10.4J impact energy, no information about the damage depth could be derived from the UT pulse echo method. Similarly, the damage morphology are different for both the UT methods.

To summarize, for all specimens, visual surface dents either in the form of indentation from the impact gun indenter or matrix cracking ranging from 5.35mm to 18.68mm were detected on the side of the impact. The phase diagram of the EMI spectrum reliably confirmed the transducer detachment from the structure when this was not observed in the other NDT methods. All the cases of UT revealed the impact damage and the bonded transducers along with the components with varying sensitivity and accuracy depending on the position of the impacts. Partially detached transducers are also be detected, as long as the introduced damage does not completely cover it. It can be observed that the damage shapes and sizes vary slightly from one another for UT through transmission as well as for UT pulse-echo methods. TT in reflection configuration can only detect damages with impact energy of approximately 13J on the damage application side. On the transducer side, structural damage of less than 13J is also detected, as long as it is not covered by the transducer. Debonding of the transducer are detected by the TT from the transducer side. Thus, the factor of accessibility has to be considered for the inspection of structures with functional elements.

4.3. Limitations

The findings of this experiment demonstrate that the use of multiple NDT methods are effective for condition monitoring and anomaly detection of multifunctional composite structures. However, some limitations of this research are:

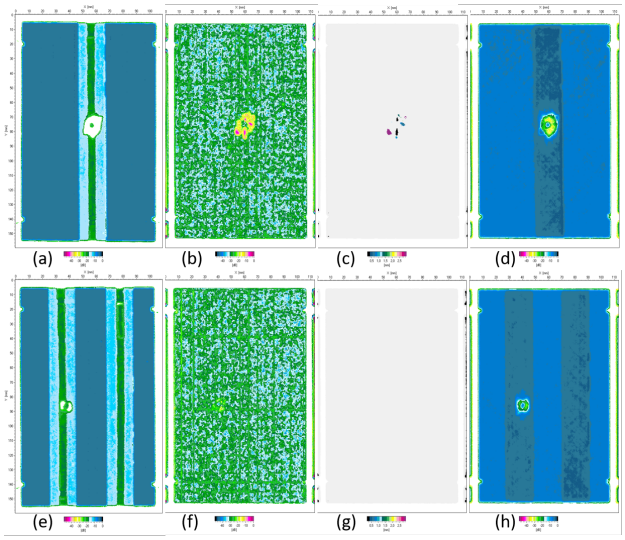

FIG 4. NDT results for specimens with conductor tracks(a) through-transmission C-scan for 21_00100, (b) pulse-echo amplitude scan for 21_00100, (c) pulse-echo damage depth scan for 21_00100, (d) pulse-echo backwall scan for 21_00100, (e) through-transmission C-scan for 22_01010 showing artificial damage, (f) pulse-echo amplitude scan for 22_01010, (g) pulse-echo damage depth scan for 22_01010, (h) pulse-echo backwall scan for 22_01010

- The sample size limitation to 16 specimens of which only two specimens were embedded the conductor tracks.
- The necessity of repetitive and consistent impact analysis would only indicate the variations in data.
- The NDT methods were limited to only three methods for inspection of the structure: UT through transmission, UT pulse-echo and TT.

5. CONCLUSION AND FUTURE SCOPE

The inspection of composite structure with functional elements using different NDT methods for the identification of impact-based damages is considered in this research. The extent to which each NDT method is suitable to detect damage, the effect of impact damage to the functional elements and the bonding between the functional element and the structure are investigated. The damage localisation and characterisation using NDT methods such as UT, VT and TT and EMI have advantages and disadvantages. They are suitable to identify damages in the structure despite the presence of functional elements bonded onto the structure. However, specific information about the size, morphology and accuracy can be efficiently estimated if the inspection data is combined using fusion techniques and in combination with referencing methods on the structure. The complementary fusion method is better for an efficient damage assessment for the structures with integrated and bonded functional elements. Further studies are required to find more practical means for the combinations of data. This may be achieved by using Digital Imaging and Communication for Nondestructive Evaluation (DICONDE) as a common data format.

6. ACKNOWLEDGMENTS

The authors would like to thank the team from the DLR project "FraME", Bernd Friederichs and Ulrich Natge for their contributions and support.

Contact address:

geo.jacob@dlr.de

References

[1] Florian Raddatz. *Lokalisierung der Interaktionsorte von Lambwellen in komplexen Faserverbundstrukturen*. PhD thesis, Institut für Faserverbundleichtbau und Adaptronik, 2016.

[2] Hakan Ucan, Joachim Scheller, Chinh Nguyen, Dorothea Nieberl, Thomas Beumler, Anja Haschenburger, Sebastian Meister, Erik Kappel, Robert Prussak, Dominik Deden, et al. Automated, quality assured and high volume oriented production of fiber metal laminates (fml) for the next generation of passenger aircraft fuselage shells. *Science and Engineering of Composite Materials*, 26(1):502–508, 2019. DOI: 10.1515/secm-2019-0031.

[3] J. Faber, A. Hindersmann, C. Bäns, S. Torstrick-von der Lieth, and F. Behrens. Innovationen für die fertigung hybrider strukturbauteile aus fml und duromer/thermoplast-hybriden. *Deutscher Luft- und Raumfahrtkongress 2023, Stuttgart*, 2023. DOI: 10.25967/610331.

[4] D. Schmidt, M. Moix-Bonet, S. Galiana, and P. Wierach. Integration von angepassten und dezentralen structural health monitoring systemen in faserverbundstrukturen. *Deutscher Luft- und Raumfahrtkongress 2023, Stuttgart*, 2023. DOI: 10.25967/610330.

[5] A. Pototzky, D. Stefaniak, and C. Hühne. Potentials of load carrying, structural integrated conductor tracks. In *47th International SAMPE Symposium and Exhibition, Books 1 and 2*, volume 47, 2017.

[6] Stelios K. Georgantzinos, Georgios I. Giannopoulos, Konstantinos Stamoulis, and Stylianos Markolefas. Composites in aerospace and mechanical engineering. *Materials*, 16(22), 2023. DOI: 10.3390/ma16227230.

[7] Bing Wang, Shuncong Zhong, Tung-Lik Lee, Kevin S Fancey, and Jiawei Mi. Non-destructive testing and evaluation of composite materials/structures: A state-of-the-

art review. *Advances in Mechanical Engineering*, 12(4):168781402091376, April 2020. DOI: 10.1177/1687814020913761.

[8] Geo Jacob and Florian Raddatz. Data fusion for the efficient ndt of challenging aerospace structures: a review. In Norbert G. Meyendorf, Christopher Niezrecki, and Saman Farhangdoust, editors, *NDE 4.0, Predictive Maintenance, and Communication and Energy Systems in a Globally Networked World*. SPIE, April 2022. DOI: 10.1117/12.2612357.

[9] Andrzej Katunin, Angelika Wronkowicz-Katunin, and Krzysztof Dragan. Impact damage evaluation in composite structures based on fusion of results of ultrasonic testing and x-ray computed tomography. *Sensors*, 20(7):1867, 2020. DOI: 10.3390/s20071867.

[10] Sanghyun Yoo, Akbar Afaghi Khatibi, and Everson Kandare. Durability of embedded pzts in structural health monitoring systems under cyclic loading. *Advanced Materials Research*, 891:1255–1260, 2014. DOI: 10.4028/www.scientific.net/AMR.891-892.1255.

[11] Andrzej Katunin, Krzysztof Dragan, and Michał Dziendzikowski. Damage identification in aircraft composite structures: A case study using various non-destructive testing techniques. *Composite structures*, 127:1–9, 2015.

[12] Christos Andreades, Michele Meo, and Francesco Ciampa. Tensile and fatigue testing of impacted smart cfrp composites with embedded pzt transducers for nonlinear ultrasonic monitoring of damage evolution. *Smart materials and structures*, 29(5):055034, 2020. DOI: 10.1088/1361-665X/ab7f41.

[13] GS Shipunov, AS Nikiforov, MA Baranov, AA Tihonova, and AA Tretyakov. The study of the possibility of x-ray inspection of fiber-optic sensors embedded into the structure of a polymer composite material. In *IOP Conference Series: Materials Science and Engineering*, volume 1100, page 012029. IOP Publishing, 2021. DOI: 10.1088/1757-899X/1100/1/012029.

[14] Amir Javidinejad and Shiv P Joshi. Design and structural testing of smart composite structures with embedded conductive thermoplastic film. *Smart materials and structures*, 8(5):585, 1999. DOI: 10.1088/0964-1726/8/5/309.

[15] Kwang Joon Yoon, Young Suk Kim, Young Bae Kim, JD Lee, Hyun Chul Park, Nam Seo Goo, and JH Lee. Parametric study on compression deformation behavior of conformal load-bearing smart skin antenna structure. *Key Engineering Materials*, 261:663–668, 2004. DOI: 10.4028/www.scientific.net/KEM.261-263.663.

[16] Hyonny Kim, Myounggu Park, and Kelli Hsieh. Fatigue fracture of embedded copper conductors in multifunctional composite structures. *Composites Science and Technology*, 66(7-8):1010–1021, 2006. DOI: 10.1016/j.compscitech.2005.08.007.

[17] Hyonny Kim and Kelli Hsieh. Measurement and prediction of embedded copper foil fatigue crack growth in multifunctional composite structure. *Composites Part A: Applied Science and Manufacturing*, 43(3):492–506, 2012. DOI: 10.1016/j.compositesa.2011.11.017.

[18] Yacine Ouroua, Said Abdi, and Imene Bachirbey. Rupture by impact-induced fatigue of a copper foil strip embedded in a multifunctional composite material. *Journal of Composite Materials*, 55(19):2631–2643, 2021. DOI: 10.1177/0021998321994327.

[19] James S. Chilles, Anastasia F. Koutsomitopoulou, Anthony J. Croxford, and Ian P. Bond. Monitoring cure and detecting damage in composites with inductively coupled embedded sensors. *Composites Science and Technology*, 134:81–88, 2016. DOI: 10.1016/j.compscitech.2016.07.028.

[20] Tianyi Feng, Dimitrios Bekas, and M. H. Ferri Aliabadi. Active health monitoring of thick composite structures by embedded and surface-mounted piezo diagnostic layer. *Sensors*, 20(12):3410, 2020. DOI: 10.3390/s20123410.

[21] G Ólafsson, RC Tighe, SW Boyd, and JM Dulieu-Barton. Development of an integrated sacrificial sensor for damage detection and monitoring in composite materials and adhesively bonded joints. *Structural Health Monitoring*, 20(6):3406–3423, 2021. DOI: 10.1177/1475921721989041.

[22] Hyonny Kim and Miguel González. Fatigue failure of printed circuit board chemically etched copper traces in multifunctional composite structures. *Journal of Composite Materials*, 48(8):985–996, 2014. DOI: 10.1177/0021998313480980.

[23] Hexcel. Hexply m21 global data sheet, 2023. Accessed: 06 July 2023.

[24] Inka Mueller and Claus-Peter Fritzen. Inspection of piezoceramic transducers used for structural health monitoring. *Materials*, 10(1):71, 2017. DOI: 10.3390/ma10010071.

[25] A Francisco G Tenreiro, António M Lopes, and Lucas FM da Silva. A review of structural health monitoring of bonded structures using electromechanical impedance spectroscopy. *Structural Health Monitoring*, 21(2):228–249, 2021. DOI: 10.1177/1475921721993419.